ENERGY DETECTORS FOR SPARSE SIGNALS

*Shahzad Gishkori, Geert Leus**

Circuits and Systems
Faculty of EEMCS, TU Delft
2628 CD Delft, The Netherlands

Hakan Deliç

Wireless Communications Laboratory
Department of EE, Boğaziçi University
Bebek 34342 Istanbul, Turkey

ABSTRACT

In this paper, compressive sampling (CS) based energy detectors are developed for sparse communication signals, namely, pulse-position modulation (PPM) and frequency shift-keying (FSK) signals so as to reduce the complexity and sampling rate at the receiver. We focus on noncoherent detection, thereby avoiding the channel estimation step. Exact bit error probability (BEP) expressions for receivers sampling at the Nyquist rate are derived to ascertain the performance of CS-based energy detectors. Simulation results provide insight into the choice of measurement matrices for a practical implementation of CS.

***Index Terms*—** Compressive sampling, pulse-position modulation, frequency shift-keying, bit error probability, measurement matrix.

1. INTRODUCTION

Digital communications has been witnessing a phenomenal growth in applications that involve signals of very high bandwidth, e.g., ultra-wideband (UWB) and frequency-hopping spread spectrum (FH-SS) signals, etc. Pulse-position modulation (PPM) and frequency shift-keying (FSK) have gained quite an importance in the realization of such systems. A big hurdle in this regard is the efficiency of the analog-to-digital converters (ADCs). According to the classical Shannon-Nyquist-Whittaker-Kotelnikov sampling theorem [1], a low-pass signal $x(t)$ (or $X(\omega) = 0, |\omega| > \omega_m$ in frequency domain) can be determined completely from its samples $x(nT)$ if $T \leq \pi/\omega_m$. The sampling rate should be at least twice the highest frequency. Therefore, if the bandwidth of the signal is too high, ADCs can be heavily stressed causing an increase in the power consumption. It could take 'decades' before the ADC technology can become fast and precise enough for the high-bandwidth applications. It is described in [1] that most of the signals with a large bandwidth have a small rate of information. This property of wideband signals makes them sparse in information and has led to methods of sampling based on the amount of information (or the rate of innovation). The combination of sparsity with finite rate of innovation is described in [2] primarily for the non-discrete domain. Compressive sampling (CS) [3, 4] offers more flexible options to deal with sparse signals in terms of the location of the information and the non-uniformity of measurements as we shall elaborate upon in subsequent sections. We take advantage of the sparsity of the PPM and FSK modulated signals, which are sparse in the time and frequency domains, respectively, through CS. In order to reduce the overall system complexity and power consumption, we concentrate on non-coherent reception of signals through energy detection.

*This work is supported in part by NWO-STW under the VICI program (project 10382).

2. SIGNAL MODEL

Let the $N \times 1$ vector $\mathbf{s}$ represent the transmitted signal in terms of its samples taken at the Nyquist rate. The signal $\mathbf{s}$ can also be represented in terms of a set of basis functions as

$$\mathbf{s} = \mathbf{B}\mathbf{a}$$

where $\mathbf{B}$ is the $N \times N$ matrix containing N basis vectors and $\mathbf{a}$ is a sparse coefficient vector with only a few nonzero elements. For PPM $\mathbf{B} = \mathbf{I}$ (identity matrix), and in case of FSK, $\mathbf{B} = \mathbf{F}^{\mathbf{H}}$ where $\mathbf{F}$ is the normalized discrete Fourier transform (DFT) matrix and F^H is its Hermitian so that $\mathbf{F}^H\mathbf{F} = \mathbf{I}$. For PPM, $\mathbf{a}$ will have a nonzero component at the beginning of a pulse. In case of a 2-PPM symbol, $a_1 = 1$ or $a_{N/2} = 1$. For FSK, each element of $\mathbf{a}$ corresponds to a carrier frequency. Therefore, its nonzero elements represent the active carriers. Let $\mathbf{h}$ be the channel response vector with L taps and $\mathbf{H}$ be the respective convolution matrix. Assuming a cyclic prefix of length $L-1$, $\mathbf{H}$ can be represented as circulant. The received signal is

$$\mathbf{x} = \mathbf{H}\mathbf{s} + \mathbf{n}$$

where $\mathbf{n}$ is the $N \times 1$ noise vector containing additive white Gaussian noise. If $\mathbf{x}$ is sparse in some basis then according to the CS theory [3, 4] it can be represented by M linear measurements with $M \ll N$. The compressed received signal is

$$\mathbf{y} = \mathbf{\Phi}\mathbf{x} \tag{1}$$

where the $M \times N$ matrix $\mathbf{\Phi}$ is the transform operator or measurement matrix with M linear functionals as its rows. For PPM, (1) can be written in the standard CS form as

$$\begin{aligned}\mathbf{y}_{\mathrm{PPM}} &= \mathbf{\Phi}\mathbf{H}\mathbf{a} + \mathbf{\Phi}\mathbf{n} \\ &= \mathbf{\Phi}\mathbf{\Psi}_{\mathrm{PPM}}\mathbf{r}_{\mathrm{PPM}} + \mathbf{\Phi}\mathbf{n}\end{aligned}$$

where $\mathbf{\Psi}_{\mathrm{PPM}} = \mathbf{I}$ and $\mathbf{r}_{\mathrm{PPM}} = \mathbf{H}\mathbf{a}$. For FSK, we can express (1) as

$$\begin{aligned}\mathbf{y}_{\mathrm{FSK}} &= \mathbf{\Phi}\mathbf{H}\mathbf{F}^H\mathbf{a} + \mathbf{\Phi}\mathbf{n} \\ &= \mathbf{\Phi}\mathbf{F}^H\mathbf{D}\mathbf{a} + \mathbf{\Phi}\mathbf{n} \\ &= \mathbf{\Phi}\mathbf{\Psi}_{\mathrm{FSK}}\mathbf{r}_{\mathrm{FSK}} + \mathbf{\Phi}\mathbf{n}\end{aligned}$$

where $\mathbf{\Psi}_{\mathrm{FSK}} = \mathbf{F}^H$ and $\mathbf{r}_{\mathrm{FSK}} = \mathbf{D}\mathbf{a}$ with the $N \times N$ diagonal matrix $\mathbf{D} := \mathbf{F}\mathbf{H}\mathbf{F}^H$ containing the eigenvalues of the channel matrix.

Thus the sampling rate (M) for the compressed signal is much less than the Nyquist rate (N) at the receiver side. For both kinds

of signals we reconstruct $\mathbf{x}$ using the orthogonal matching pursuit (OMP) [5] and basis pursuit (BP) algorithms. We shall apply our detection rules on $\hat{\mathbf{x}}$ (the reconstructed $\mathbf{x}$) which will lead to a decision on $\mathbf{s}$ or $\mathbf{a}$.

3. ENERGY DETECTION OF PPM

In order to reduce the overall system complexity and power consumption, we concentrate on noncoherent reception of PPM signals, which is akin to a generalized maximum likelihood (GML) detector [6]. The symbol decision is based on finding the pulse position that contains the maximum energy. The symbol-by-symbol detection process does not require the estimation of the channel parameters. The energies of the multipath components are combined to increase the detection probability of the actual transmitted pulse.

Let us focus on 2-PPM for simplicity. The symbol vector $\mathbf{s}$ contains the pulse in the first or second half. The received signal vector $\mathbf{x}$ shall reflects the same situation but with increased energy as a result of the accumulation of multipath components. We consider two kinds of detection scenarios: (i) the quasi-synchronous case in which the exact start of the received pulse is not known exactly; and (ii) the fully-synchronous case in which it is known perfectly. Assuming that the signal spread $L \ll N/2$, the starting point for the quasi-synchronous signal detection can be written as

$$0 \leq i_0 \text{ and } i_0 + L - 1 \leq N/2 - 1,$$

$$N/2 \leq i_1 \text{ and } i_1 + L - 1 \leq N - 1$$

where i_0 represents the starting point if symbol 0 was transmitted and i_1 if symbol 1 was transmitted. For the received signal sampled at Nyquist-rate, the quasi-synchronous decision rule is

$$u_1 = \sum_{i=0}^{N/2-1} x_i^2 \underset{1}{\overset{0}{\gtrless}} u_2 = \sum_{i=N/2}^{N-1} x_i^2, \tag{2}$$

while for the fully-synchronous case, the rule is

$$u_1 = \sum_{i=0}^{L-1} x_i^2 \underset{1}{\overset{0}{\gtrless}} u_2 = \sum_{i=N/2}^{N/2+L-1} x_i^2. \tag{3}$$

We apply the similar detection rule on the received signal reconstructed from compressed samples, i.e., $\hat{\mathbf{x}}_{\mathrm{PPM}}$. In this way we compare the performance of our CS-based energy detector with the one which is sampled at Nyquist rate. In the following, we derive the theoretical performance of the detectors (2) and (3) for Nyquist-rate sampling to provide us a benchmark for CS-based detectors.

3.1. Quasi-Synchronous Detector

We assume that the channel and noise coefficients, h_i and n_i, are independent and identically distributed (i.i.d.) Gaussian random variables such that $h_i \sim \mathcal{N}(0,1)$ and $n_i \sim \mathcal{N}(0,\sigma^2)$ for $i = 0, 1, \ldots, N-1$. Assuming that a zero is transmitted, we can write $x_i = (h_i + n_i) \sim \mathcal{N}(0, 1+\sigma^2)$ for $i = 0, 1, \ldots, N-1$.

From (2), we can write the BEP for the case where a zero is transmitted as

$$P_e = P(u_1 < u_2 | 0 \text{ is sent}),$$

where $u_1 = \sum_{i=0}^{N/2-1}(h_i + n_i)^2$ and $u_2 = \sum_{i=N/2}^{N-1} n_i^2$. Since $L < N/2$, u_1 can be written as

$$u_1 = \sum_{i=0}^{L-1}(h_i + n_i)^2 + \sum_{i=L}^{N/2-1} n_i^2.$$

Let $u_{1a} = \sum_{i=0}^{L-1}(h_i+n_i)^2$ and $u_{1b} = \sum_{i=L}^{N/2-1} n_i^2$. The probability density functions (pdfs) of these chi-square random variables can be written as [9]

$$p_{U_{1a}}(u_{1a}) = \frac{{u_{a1}}^{\frac{L}{2}-1}}{\sigma_1^L 2^{\frac{L}{2}}\Gamma\left(\frac{L}{2}\right)} e^{\frac{-u_{1a}}{2\sigma_1^2}},$$

$$p_{U_{1b}}(u_{1b}) = \frac{{u_{1b}}^{\frac{N-2L}{4}-1}}{\sigma_2^{(N-2L)/2} 2^{\frac{N-2L}{4}}\Gamma\left(\frac{N-2L}{4}\right)} e^{\frac{-u_{1b}}{2\sigma_2^2}}$$

where $\sigma_1^2 = 1+\sigma^2$ and $\sigma_2^2 = \sigma^2$. The pdf of u_1 is

$$p_{U_1}(u_1) = \int_0^\infty p_{U_{1a}}(u_{1a}) p_{U_{1b}}(u_1 - u_{1a}) du_{1a}. \tag{4}$$

Using [7, Eq. (5.26)], a solution of (4) can be written as

$$p_{U_1}(u_1) = \frac{1}{2\sigma_1\sigma_2\Gamma(\frac{N}{4})}\left[\frac{u_1}{2\sigma_1^2}\right]^{\frac{L-1}{2}}\left[\frac{u_1}{2\sigma_2^2}\right]^{\frac{N-2L-2}{2}} \times e^{\frac{-u_1}{2\sigma_2^2}}\, {}_1F_1\left[\frac{L}{2}, \frac{N}{4}; \frac{(\sigma_2^2-\sigma_1^2)^2}{2\sigma_1^2\sigma_2^2}u_1\right],$$

where ${}_1F_1[.,.;.]$ is the Kummer confluent hypergeometric function which is defined in [8, Eq. (9.210.1)]. The pdf of u_2 can be written as [9]

$$p_{U_2}(u_2) = \frac{{u_2}^{\frac{N}{4}-1}}{\sigma_w^{N/2} 2^{\frac{N}{4}}\Gamma\left(\frac{N}{4}\right)} e^{\frac{-u_2}{2\sigma_w^2}}$$

where $\sigma_w^2 = \sigma^2$. The probability of a correct decision given u_1 and given that a zero is transmitted can then be written as

$$P_c = P(u_2 < u_1 | u_1) = \int_0^{u_1} p_{U_2}(u_2)\, du_2$$
$$= \int_0^{u_1} \frac{{u_2}^{\frac{N}{4}-1}}{\sigma_w^N 2^{\frac{N}{4}}\Gamma\left(\frac{N}{4}\right)} e^{\frac{-u_2}{2\sigma_w^2}} du_2 = \frac{\gamma\left(\frac{N}{4}, \frac{u_1}{2\sigma_w^2}\right)}{\Gamma\left(\frac{N}{4}\right)},$$

where $\Gamma(.)$ is the gamma function and $\gamma(.,.)$ is the lower-incomplete-gamma function such that $\gamma(n,u) = \int_0^u t^{n-1}e^{-t}dt$ [8]. The average BEP for the quasi-synchronous PPM detector is

$$P_e = 1 - \int_0^\infty P_c p_{U_1}(u_1) du_1$$
$$= 1 - \int_0^\infty \frac{\gamma\left(\frac{N}{4}, \frac{u_1}{2\sigma_w^2}\right)}{\Gamma\left(\frac{N}{4}\right)} p_{U_1}(u_1) du_1. \tag{5}$$

Because (5) is not in closed form, it has to be solved numerically.

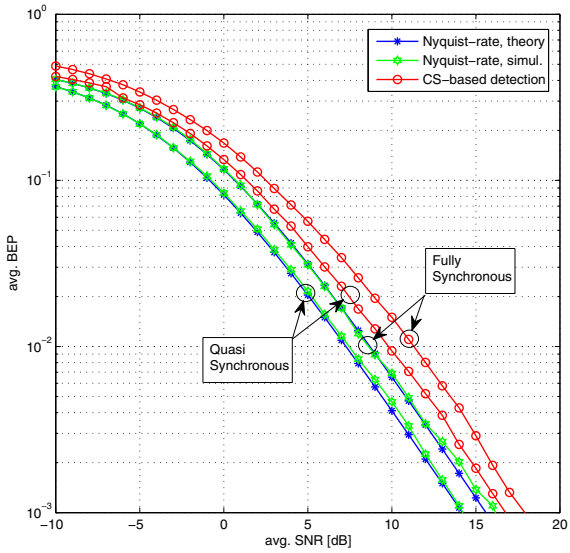

Fig. 1. Average BEP of 2-PPM with $L = 3$ taps, measurement matrix = DFT matrix, reconstruction algorithm = OMP.

3.2. Fully-Synchronous Detector

In this subsection we present the average BEP expression for fully-synchronous PPM detector in closed form. We have similar assumptions for the channel and noise distributions as in Subsection 3.1 with the difference that now we are aware of the exact start of the received pulse. From (3), we can write the BEP for the case a zero is transmitted as

$$P_e = P(u_1 < u_2 | 0 \text{ is sent}),$$

where $u_1 = \sum_{i=0}^{L-1}(h_i + n_i)^2$ and $u_2 = \sum_{i=N/2}^{N/2+L-1} n_i^2$. Following the steps in 3.1, the average BEP expression for this case can be found as

$$P_e = 1 - \frac{2\Gamma(L)}{L[\Gamma(\frac{L}{2})]^2}\left[\frac{\sigma_1\sigma_2}{\sigma_1^2+\sigma_2^2}\right]^L {}_2F_1\left(1, L; \frac{L}{2}+1; \frac{\sigma_1^2}{\sigma_1^2+\sigma_2^2}\right)$$

where ${}_2F_1(.,.;.;.)$ is the Gaussian hypergeometric function that is defined by [8, Eq. (9.14.2)].

3.3. Simulation Results

In this subsection, we present the performance results of our CS-based energy detector for 2-PPM signals. We consider a channel of length $L = 3$. Since we have assumed a zero-mean Gaussian distributed channel with variance one, the average channel energy is

$$\bar{E}_h = E\left\{\sum_{i=0}^{L-1} h_i^2\right\} = L,$$

the average singal-to-noise ratio (SNR) is defined as

$$\bar{\eta}_{\text{PPM}} = \frac{\bar{E}_h}{N\sigma^2} = \frac{L}{N\sigma^2}$$

where N is the number of Nyquist-rate samples of a PPM symbol. Figure 1 shows the results of our PPM detector. We can see that the theoretical curves are closely followed by the Nyquist-rate detection. For the CS-based detector, we assume a compression ratio of 50 per cent with $N = 8$ and $M = 4$. We use a DFT matrix as the measurement matrix ($\mathbf{\Phi}$) and OMP as the reconstruction algorithm. We observe a moderate average SNR loss of about 2-3 dB for both quasi- and fully-synchronous CS-based detection. Figure 2 shows the performance of the quasi-synchronous detector for the case when the measurement matrix is Gaussian matrix and the reconstruction is with OMP, as well as BP. Both algorithms are not able to give a good performance when a Gaussian matrix is used as the measurement matrix. It should be noted that the order of sparsity for this example is $K = L = 3$. When we reduce the order of sparsity to $K = 1$, we find a better performance within this set-up. Similarly keeping $K = 3$ and increasing N (while $M/N = 0.5$) also results in a better performance. This means that the performance of Gaussian measurement matrices depends both on the order of sparsity and the value of N. In general, we have found in many simulations that when $M/N = 0.5$, the relationships $K \leq 0.044708N$ [11] and $K \leq 0.0016N$ [12] hold true for good-to-best performing Gaussian measurement matrices, as well as other random matrices. Thus, according to [11], we have $N \geq 67$ for $K = 3$, and according to [12], it is $N \geq 1875$ for $K = 3$. These relations provide a lower bound on N for a given order of sparsity and can also be modified to represent an upper bound on K for a given value of N.

These observations highlight some very important aspects of CS when used in practical communication environments. In most of CS theory, Gaussian (or other random matrices) are presented as a favorable choice but this mostly holds in the asymptotic sense as $N \to \infty$ [3]. It is in this context that the random matrices exhibit restricted isometry property (RIP) [4] and the number of measurements required for exact reconstruction with high probability are $M \propto K\log(N/K)$. In the field of communications this may not be always realizable since N is limited because of the signal properties and/or processing complexity. Thus, structured matrices such as the DFT matrix may perform better as is clear from Figure 1.

4. ENERGY DETECTION OF FSK

For FSK we use noncoherent energy detection and thereby circumvent the complications of phase estimation, which leads to further simplification of the detection process. We consider single-tone (i.e., one carrier is active at a time) and dual-tone (i.e., two carriers are active) FSK. Single-tone FSK is frequently used in FH communication. Dual-tone FSK has been presented in literature (e.g., [10]) as a solution for limited frequency bands to improve multiple access performance in FH-SS. The benefit of dual-tone is in terms of the ability to increase multiple access but at the same time, the tone energy is half of that of the conventional FSK. Therefore, dual-tone trades noise performance for multiple access enhancement [10].

The decision process boils down to finding one or two coefficients (for single- or dual-tone, respectively) in $\mathbf{a}$ which contain maximum energy since the elements of $\mathbf{a}$ correspond to the N carrier frequencies. Similar to PPM, a decision on $\mathbf{x}$ (for the non-CS) and $\hat{\mathbf{x}}_{\text{FSK}}$ can lead to a decision on $\mathbf{a}$. Since $\mathbf{x}_{\text{FSK}} = \mathbf{Da}$, we can exclude the process of channel estimation. $\mathbf{x}_{\text{FSK}}$ would be 1-sparse for single-tone FSK and 2-sparse for dual-tone FSK. The decision criterion on the elements of $\mathbf{x}$ for the case of single-tone FSK is

$$d = \arg \max_{i \in \{1,\ldots,N\}} \|x_i\|_2^2 \qquad (6)$$

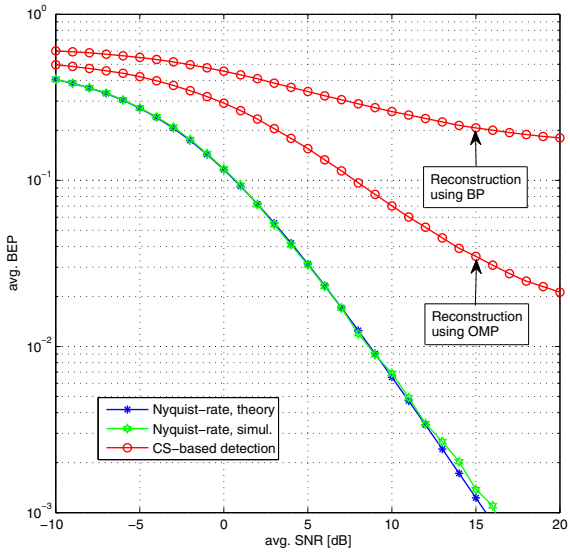

Fig. 2. Average BEP of 2-PPM with $L = 3$ taps, measurement matrix = Gaussian matrix, reconstruction algorithms = OMP and BP.

where d is the decision variable and for the dual-tone FSK it is

$$d' = \arg \max_{\substack{i,j:\in\{1,\ldots,N\} \\ i\neq j}} \sum_{i,j} \left(\|x_i\|_2^2 + \|x_j\|_2^2 \right).$$

For the dual-tone $N(N-1)/2$ unique combinations are possible where each combination consists of two frequency bands [10]. Since these combinations can potentially produce dependent variables, we consider only independent combinations to derive the theoretical BEP expressions for the sake of simplicity. We consider the $N/2$ combinations with two consecutive tones, and compare the energies of these combinations so that the detection rule is

$$d'' = \arg \max_{(i,j)\in\{(1,2),(3,4),\ldots,(N-1,N)\}} \sum_{i,j} \left(\|x_i\|_2^2 + \|x_j\|_2^2 \right). \quad (7)$$

Similar detection rules are applied to $\hat{\mathbf{x}}_{\text{FSK}}$ for the CS-based FSK energy detectors. In the following, we derive the theoretical performance of these detectors, i.e., (6) and (7) for Nyquist-rate sampling to provide us a benchmark for CS-based detectors.

4.1. Single-Tone Detector

We assume that the channel coefficients are Rayleigh distributed with unit-variance, and the noise components n_i are i.i.d. zero-mean Gaussian distributed with variance σ^2, for $i = 1, \ldots, N$. Supposing that the first carrier was transmitted, define $u_1 = \left\| h_1 e^{-j\phi_1} + n_1 \right\|_2^2$ and $u_i = \|n_i\|_2^2$ where h_1 is the respective diagonalized channel coefficient and ϕ_1 is the respective carrier phase. The pdfs of these variables can be derived to be

$$p_{U_1}(u_1) = \frac{e^{\frac{-u_1}{2\sigma_1^2}}}{2\sigma_1^2}, \quad (8)$$

$$p_{U_i}(u_i) = \frac{e^{\frac{-u_i}{2\sigma_2^2}}}{2\sigma_2^2} \quad (9)$$

where $\sigma_1^2 = L + \sigma^2$ and $\sigma_2^2 = \sigma^2$ [9]. The probability of correct decision in comparison to the ith carrier, given that the first carrier was transmitted, is

$$P_{c_i} = P\left(u_i < u_1 | u_1, \text{first carrier}\right) = \int_0^{u_1} p_{U_i}(u_i)\, du_i$$
$$= \frac{1}{2\sigma_2^2} \int_0^{u_1} e^{\frac{-u_i}{2\sigma_2^2}}\, du_i = 1 - e^{\frac{-u_1}{2\sigma_2^2}}.$$

If all decision variables u_i, $i = 2, \ldots, N$, are i.i.d., we can write the correct probability for the joint pdf as

$$P_c = P\left(\bigcap_{i=2}^{N} u_i < u_1 | u_1, \text{first carrier} \right) = \left[1 - e^{\frac{-u_1}{2\sigma_2^2}} \right]^{N-1}$$

and the BEP can be derived as

$$P_e = 1 - \int_0^{\infty} P_c p_{U_1}(u_1)\, du_1$$
$$= 1 - \frac{1}{2\sigma_1^2} \int_0^{\infty} \left[1 - e^{\frac{-u_1}{2\sigma_2^2}} \right]^{N-1} e^{\frac{-u_1}{2\sigma_1^2}}\, du_1.$$

Using [8, Eq. (3.312)], it can be simplified in the following closed form

$$P_e = 1 - \frac{\sigma_2^2}{\sigma_1^2} B\left(\frac{\sigma_2^2}{\sigma_1^2}, N \right)$$

where $B(.,.)$ is the beta function [8].

4.2. Dual-Tone Detector

For dual-tone, we use similar assumptions on the channel and the noise as in subsection 4.1. Because two carriers are transmitted, we need to find two consecutive elements of $\mathbf{x}$ which give the maximum energy according to (7). Given that the first two carriers are transmitted, define $u_1 = \sum_{i=1}^{2} \left\| h_i e^{-j\phi_i} + n_i \right\|_2^2$, and the variable for any other combination, $u_q = \sum_{k=q}^{q+1} \left\| h_k e^{-j\phi_k} + n_k \right\|_2^2$ for $q \in \mathcal{Q} = \{3, 5, 7, \ldots, N-3, N-1\}$ with $|\mathcal{Q}| = N/2 - 1$. The pdfs of these variables are similar to (8) and (9) but with twice their degrees of freedom, i.e.,

$$p_{U_1}(u_1) = \frac{u_1 e^{\frac{-u_1}{2\sigma_1^2}}}{4\sigma_1^4},$$

$$p_{U_q}(u_q) = \frac{u_q e^{\frac{-u_q}{2\sigma_2^2}}}{4\sigma_2^4}.$$

The probability of correct decision given that the carriers of decision variable u_1 were transmitted is

$$P_{c_q} = P\left(u_q < u_1 | u_1, \text{first two carriers}\right) = \int_0^{u_1} p_{U_q}(u_q)\, du_q$$
$$= \frac{1}{4\sigma_2^4} \int_0^{u_1} u_q e^{\frac{-u_q}{2\sigma_2^2}}\, du_q, q \in \mathcal{Q}.$$

Using [8, Eq. (3.351.1)], it simplifies to

$$P_{c_q} = 1 - e^{\frac{-u_1}{2\sigma_2^2}} \left(1 + \frac{u_1}{2\sigma_2^2}\right).$$

If all the decision variables u_q are i.i.d., we can write the correct decision probability for the joint pdf as

$$\begin{aligned} P_c &= P\left(\bigcap_{q\in\mathcal{Q}} u_q < u_1 | u_1, \text{first two carriers}\right) \\ &= \left[1 - e^{\frac{-u_1}{2\sigma_2^2}} \left(1 + \frac{u_1}{2\sigma_2^2}\right)\right]^{N/2-1}. \end{aligned}$$

The average BEP can then be found as

$$\begin{aligned} P_e &= 1 - \int_0^\infty P_c p_{U_1}(u_1) du_1 \\ &= 1 - \int_0^\infty \left[1 - e^{\frac{-u_1}{2\sigma_2^2}} \left(1 + \frac{u_1}{2\sigma_2^2}\right)\right]^{N/2-1} p_{U_1}(u_1) du_1. \end{aligned}$$

4.3. Simulation Results

We consider 8-FSK with $L = 3$ Rayleigh distributed channel taps. The average SNR can be written as $\bar{\eta}_{\text{FSK}} = L/m\sigma^2$ where $m = \log_2 N$. Figure 3 shows simulation results for both single- and dual-tone FSK energy detection, validating the analytical expressions. For the CS-based detection we use $M = 4$ and a Gaussian measurement matrix in case of single-tone, and $M = 6$ and identity matrix as the measurement matrix for the dual-tone. Despite the multipath effects, the order of sparsity is $K = 1$ for the single-tone and $K = 2$ for the dual-tone FSK because of the diagonalization of the circulant channel matrix $\mathbf{H}$ as described earlier. We see that Gaussian matrix does a good job for the single-tone but for higher order of sparsity we have to resort to a structured matrix (identity matrix in this case) for comparatively better performance. Therefore, the observations regarding the measurement matrices described in Section 3.3 hold true. For simulations of Nyquist-rate detection of dual-tone FSK, correlated carriers are employed. This explains the gap between the simulation results and the theoretical Nyquist-rate average BEP curves, whose derivation considered independent carriers.

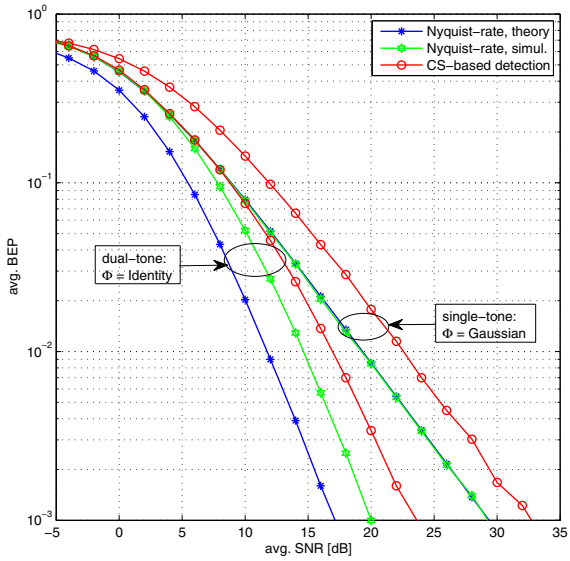

Fig. 3. Average BEP versus average SNR of single-tone and dual-tone 8-FSK ($N = 8$) with $L = 3$ taps, recon. algorithm = OMP.

5. CONCLUSION

We have presented CS-based energy detectors for PPM and FSK modulated signals in multipath fading. The receivers do not require channel estimation and the sampling rate is much below the Nyquist-rate. We provide exact analytical BEP expressions to ascertain the performance of the detectors, which were validated by simulation results. Our results provide insight into the choice of measurement matrices. We show that the random matrices are not always the best choice for practical communication scenarios.

6. REFERENCES

[1] M. Vetterli, P. Marziliano and T. Blu, "Sampling Signals with Finite Rate of Innovation," *IEEE Transactions on Signal Processing*, Vol. 50, No. 6, pp. 1417-1428, June 2002.

[2] T. Blu, P. L. Dragotti, M. Vetterli, P. Marziliano, and L. Coulot, "Sparse Sampling of Signal innovations," *IEEE Signal Proc. Mag.*, pp. 31-40, March 2008.

[3] D. L. Donoho, "Compressed Sensing," *IEEE Transactions on Information Theory*, Vol. 52, No. 4, April 2006.

[4] E. Candès, J. Romberg and T. Tao, "Robust Uncertainty Principles: Exact Signal Reconstruction from Highly Incomplete Frequency Information," *IEEE Transactions on Information Theroy*, Vol. 52, No. 2, pp. 489-509, February 2006.

[5] J. A. Tropp and A. C. Gilbert, "Signal Recovery From Random Measurements via Orthogonal Matching Pursuit," *IEEE Trans. on Info. Theory*, Vol. 53, No. 12, December 2007.

[6] C. Carbonelli and U. Mengali, "M-PPM Noncoherent Receivers for UWB Applications," *IEEE Transactions on Wireless Communications*, Vol. 5, No. 8, pp. 2285-2294, Aug. 2006.

[7] M. K. Simon, *Probability Distributions Involving Gaussian Random Variables: A Handbook for Engineers and Scientists*, New York, NY: Springer, 2006.

[8] I. S. Gradshteyn and I. M. Ryzhik, *Table of Integrals, Series, and Products*, 6th ed. San Diego, CA: Academic Press, 1996.

[9] J. G. Proakis, *Digital Communications*, 4th ed. Avenue of Americas, NY: McGraw-Hill, 2001.

[10] T. A. Gulliver and S. H. C. Ting, "Dual-Tone MFSK for Frequency-Hopped Spread-Spectrum Multiple Access Communications," *Contemporary Engineering Sciences*, Vol. 1, No. 4, pp. 177-191, 2008.

[11] D. L. Donoho, *High-Dimensional Centrally-Symmetric Polytopes with Neighborliness Proportional to High Dimension*, Technical Report, Stanford University, January 2005.

[12] M. Stojnic, X. Weiyu and B. Hassibi, "Compressed Sensing-Probabilistic Analysis of a Null-Space Characterization," *Proc. of ICASSP*, pp. 3377-3380, Apr. 2008.